

Article

An Earlier Spring Phenology Reduces Vegetation Growth Rate during the Green-Up Period in Temperate Forests

Boheng Wang¹, Zunchi Liu^{2,*}, Ji Lu^{1,*}, Mao Cai¹, Chaofan Zhou³, Gaohui Duan⁴, Peng Yang¹ and Jinfeng Hu⁵

¹ East China Survey and Planning Institute of National Forest and Grassland Administration, Hangzhou 310019, China; vancywang@126.com (B.W.)

² College of Water Sciences, Beijing Normal University, Beijing 100875, China

³ Key Laboratory of Forest Ecology and Environment of the National Forestry and Grassland Administration, Ecology and Nature Conservation Institute, Chinese Academy of Forestry, Beijing 100085, China

⁴ College of Grassland Agriculture, Northwest A&F University, Xianyang 712100, China

⁵ Shandong Zhengyuan Digital City Construction Co., Ltd., Jinan 264003, China

* Correspondence: zcliu2818@bnu.edu.cn (Z.L.); luji029@outlook.com (J.L.)

Abstract: Climatic warming advances the start of the growing season (SOS) and sequentially enhances the vegetation productivity of temperate forests by extending the carbon uptake period and/or increasing the growth rate. Recent research indicates that the vegetation growth rate is a main driver for the interannual changes in vegetation carbon uptake; however, the specific effects of an earlier SOS on vegetation growth rate and the underlying mechanisms are still unclear. Using 268 year-site PhenoCam observations in temperate forests, we found that an earlier SOS reduced the vegetation growth rate and mean air temperature during the green-up period (i.e., from the SOS to the peak of the growing period), but increased the accumulation of shortwave radiation during the green-up period. Interestingly, an earlier-SOS-induced reduction in the growth rate was weakened in the highly humid areas (aridity index ≥ 1) when compared with that in the humid areas (aridity index < 1), suggesting that an earlier-SOS-induced reduction in the growth rate in temperate forests may intensify with the ongoing global warming and aridity in the future. The structural equation model analyses indicated that an earlier-SOS-induced decrease in the temperature and increase in shortwave radiation drove a low vegetation growth rate. Our findings highlight that the productivity of temperate forests may be overestimated if the negative effect of an earlier SOS on the vegetation growth rate is ignored.

Keywords: climate change; digital imagery; growth rate; spring phenology; temperate forests



Citation: Wang, B.; Liu, Z.; Lu, J.; Cai, M.; Zhou, C.; Duan, G.; Yang, P.; Hu, J. An Earlier Spring Phenology Reduces Vegetation Growth Rate during the Green-Up Period in Temperate Forests. *Forests* **2023**, *14*, 1984. <https://doi.org/10.3390/f14101984>

Academic Editor: Romà Ogaya

Received: 31 August 2023

Revised: 28 September 2023

Accepted: 29 September 2023

Published: 1 October 2023



Copyright: © 2023 by the authors. Licensee MDPI, Basel, Switzerland. This article is an open access article distributed under the terms and conditions of the Creative Commons Attribution (CC BY) license (<https://creativecommons.org/licenses/by/4.0/>).

1. Introduction

As one of the most sensitive bio-indicators of climate change, the start of the growing season (SOS) has been widely advanced by climatic warming in temperate forests and is expected to further advance under ongoing warming [1,2]. The advanced SOS has multiple feedbacks to Earth systems (e.g., carbon, water, and energy exchange) via changing the vegetation growing season and/or physiological processes (e.g., growth rate) [3]. The green-up period (i.e., from the SOS to the peak of the growing season) plays a crucial role in plant growth and ecosystem productivity [4]. For example, an earlier-SOS-induced increase in the carbon absorption during the green-up period by climatic warming compensates for late-season respiration, and then dominates terrestrial ecosystem carbon storage [5,6]. Therefore, it is important to deeply understand how an earlier SOS influences the vegetation growth during the green-up period.

The interannual changes in vegetation productivity during the green-up period are jointly controlled by the length of the green-up period and the growth rate during the green-up period [7]. Recent research has proved that the maximum carbon uptake rate

can explain 78% of the interannual variation of terrestrial gross primary productivity. This implies that the vegetation growth rate has a more important role than the length of the green-up period in regulating the vegetation productivity during the green-up period [8,9]. Climate change leads to an earlier SOS and a higher vegetation carbon uptake during the green-up period at the temporal scale, indicating that an earlier SOS may increase the vegetation growth rate during the green-up period at the decadal time scale [10,11]. The interannual variation in the SOS is larger than that in the time trends [12]. Therefore, exploring the effects of an SOS on vegetation growth rate at the interannual scale could give us new insight into predicting the effects of continued advancing of the SOS on the growth rate [13]. However, whether an earlier SOS induced a higher vegetation growth rate at the interannual scale needs to be further verified, especially in various arid areas [14].

The temperature and soil water availability are the primary driving factors for plant growth [15,16]. The aridity index reflects the simultaneous changes in temperature and water availability [15]. In arid areas, the water availability is a primary limiting factor for plant growth [17]. An earlier SOS may exacerbate soil water stress, and reduce vegetation growth rate in arid areas with a low aridity index [18,19]. Conversely, the temperature is a primary limiting factor for plant growth in cold and humid areas [20]. Climate warming may have positive effects on the vegetation growth rate [14,20]. The underlying mechanisms of the changes in the vegetation growth rate are different among various arid areas [21]. However, to our knowledge, it is not known how an earlier SOS affects the vegetation growth rate across various arid areas.

In recent decades, the temperate forest phenology has been significantly altered by climatic warming, resulting in a high net carbon uptake [4]. Here, we explored the effects of an earlier SOS on the vegetation growth rate during the green-up period, and the underlying mechanisms across various arid areas in temperate forests using 268 year-site PhenoCam observations at 33 sites. Specifically, we first tested the hypothesis that an earlier vegetation growth implies lower temperature and soil water availability during the growing period [18,22], and these may slow down the vegetation growth rate, especially in arid areas [14]. Then, we tested the direct effects of an earlier SOS on the growth rate and its indirect effects via climate factors (i.e., radiation, temperature, and soil water content) using structural equation models.

2. Materials and Methods

2.1. Dataset

To explore the effects of an earlier SOS on vegetation growth rate at the interannual scale, the canopy greenness data was downloaded from PhenoCam Dataset v2.0 (https://daac.ornl.gov/VEGETATION/guides/PhenoCam_V2.html, accessed on 1 March 2023) [23]. The canopy greenness (Green Chromatic Coordinate, GCC) is extracted from the RGB imagery of digital repeat photography and is used to quantify phenological changes [24,25]. The GCC of the region of interest is expressed as follows: $GCC = G_{DN} / (R_{DN} + G_{DN} + B_{DN})$, where R_{DN} , G_{DN} , and B_{DN} are the average red, green, and blue digital numbers across the ROI, respectively. According to previous research, the daily GCC of the 90th value in the dataset was selected to minimize the effect of light [26]. In total, 33 PhenoCam sites with a total of 268 year-site records were selected according to the following standard protocols: (1) The PhenoCam site is located in the temperate forests; (2) each site has at least 7 years of available data; (3) the vegetation exhibits an obvious seasonality and only has a single growing season. The vegetation of the above selected sites was classified into two functional types according to the classification set by the International Geosphere-Biosphere Programme (IGBP): 26 DBF sites (site-years = 217), and 7 ENF sites (site-years = 51). A detailed description of each site can be found in Figure 1 and Supplementary Table S1.

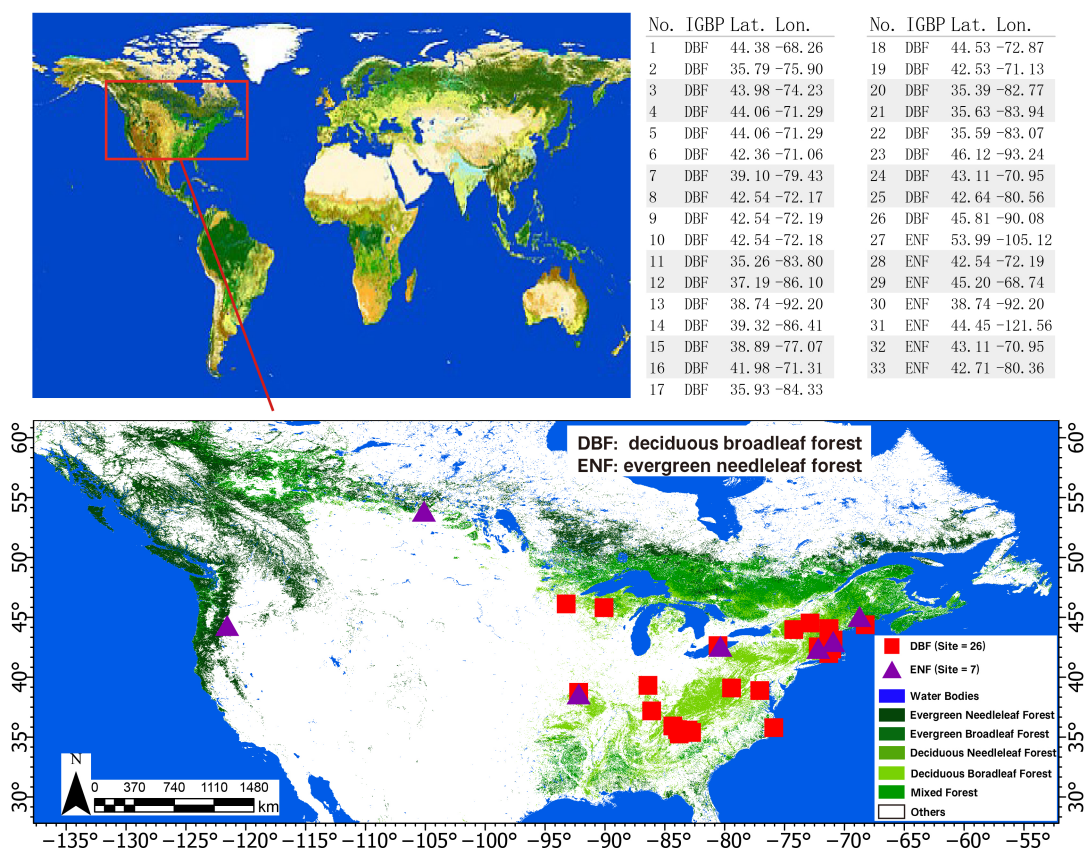


Figure 1. Distribution of study sites. All data are derived from PhenoCam dataset (https://daac.ornl.gov/VEGETATION/guides/PhenoCam_V2.html, accessed on 1 March 2023).

To extract vegetation phenology from the GCC values, three common methods ('Spline', 'Klosterman', and 'Gu') were used to reconstruct GCC time series to capture the seasonal behavior and to reduce the effect of outlier observations [27,28]. To explore the effects of SOS on vegetation growth rate during the green-up period, we estimated the SOS date using the relative threshold and inflection point methods. Specifically, for the 'Spline' and 'Gu' methods, the date when GCC values reached 20% of the annual amplitude of the fitted curve was defined as SOS [7,11]. For the 'Klosterman' method, the SOS date was determined when the GCC value increased at the fastest rate in the fitted curve [28]. The date when the maximum value occurred in the fitted seasonal curve was defined as the peak of the growing season (POS). The length of the green-up period (LGP) was then calculated as the interval between SOS and POS. Vegetation aboveground productivity during the green-up period was defined as the difference between the GCC values at POS and SOS. The growth rate during the green-up period was estimated by the following function [7]: $GR = (GCC_{POS} - GCC_{SOS}) / LGP$, where GR indicates vegetation growth rate during the green-up period. GCC_{POS} and GCC_{SOS} represent the GCC value at POS and SOS, respectively. LGP refers to the length of the green-up period. Finally, all variables were extracted/calculated from each fitted curve, and then each variable from three fitted methods was averaged to reduce uncertainties and bias caused by any single curve-fitting algorithm. To verify and ensure the robustness of the results, we also extracted the SOS value based on the 30% relative threshold for the 'Spline' and 'Gu' methods [17,25], and all variables were also calculated using the same method by the above description.

2.2. Climate Dataset

Shortwave radiation (SR), air temperature (Ta), and soil water content (SWC) of hourly grid datasets during the study period with a spatial resolution of $0.1^\circ \times 0.1^\circ$ for northern ecosystems were obtained from ERA5-land hourly data (<https://cds.climate.copernicus>).

[eu/cdsapp#!/dataset/reanalysis-era5-land?tab=overview](https://cdsapp#!/dataset/reanalysis-era5-land?tab=overview), accessed on 1 March 2023). We used the variables: ‘surface solar radiation downwards’, ‘2 m temperature’, and ‘volumetric soil water layers 1 and 2’ (0 to 28 cm). All climate factors were converted to daily scale from the hourly data. The accumulative SR during the green-up period, mean daily Ta during the green-up period, and mean daily SWC during the green-up period of each site were calculated based on the information on SOS and POS from the PhenoCam dataset.

Aridity index (AI), defined as the ratio of annual precipitation to annual potential evapotranspiration, is a widely used index to assess variation in aridity [15]. It provides a measure of water availability for potential vegetation growth and allows for both spatial and temporal comparisons. The AI of each site was obtained from Global-AI_PET_v3 dataset (https://figshare.com/articles/dataset/Global_Aridity_Index_and_Potential_Evapotranspiration_ET0_Climate_Database_v2/7504448/4, accessed on 1 March 2023), with a high-resolution (30 arc-seconds) for the 1970–2000 period [29]. According to the previous research [30,31], the AI was used to explore the effects of SOS on growth rate and climate factors along the aridity gradient. Here, lower AI values correspond to more arid climate conditions.

2.3. Statistical Analyses

All data were analyzed using R version 4.2.3 (The R Project for Statistical Computing, <https://www.r-project.org/>, accessed on 1 March 2023). We removed all outliers, which are defined as the values exceeding ± 3 standard deviations of multi-year mean values for the time series data of each variable, from each site. We implemented a 3-step protocol to analyze the data. First, the slopes and significant levels of GR, SR, Ta, SWC, and SOS; and SR, Ta, SWC, and GR were evaluated by *lm* function for each site of the PhenoCam dataset, respectively. We also calculated the yearly anomalies (Z-scores) of all variables for each site, and the correlations between yearly anomalies of SOS (Z_SOS)/GR (Z_GR) and other variables were estimated for all sites.

Second, the sites belong to humid areas when $0.65 \leq AI < 1$ and highly humid areas when $1 \leq AI < 1.5$. The study sites were classified into humid areas ($0.65 \leq AI < 1$), and highly humid areas ($1 \leq AI < 1.5$) based on the United Nations Environment Programme. The aridity index values for the sites of our study are from 0.57 to 1.51, and almost all sites (94%) are from 0.65 to 1.5. Thus, we divided the study sites into two aridity levels: humid areas ($AI < 1$), and highly humid areas ($1 \leq AI$) in this study. To explore the changes in the effects of SOS on each variable or climate factors on GR along aridity levels, the site-level slopes of the correlations between SOS/GR and variables with aridity index of different arid areas were analyzed by ordinary least squares for each vegetation type.

Third, structural equation models (SEMs) were used to distinguish between direct and indirect effects using ‘mediator’ variables [32]. The direct effect of SOS on GR, and indirect effects via SR, Ta, and SWC were determined based on theoretical and empirical knowledge (Figure S1) using the *piecewiseSEM* package of R [33]. In the SEM model, we hypothesized that SOS is likely to indirectly influence the GR because an earlier SOS can directly alter the environmental context (i.e., climate factors) of vegetation growth and determine the GR, indicated by the arrows from SOS indirectly pointing to the GR via climate factors. Correspondingly, the direct effect of SOS on GR also was tested by the arrows from SOS directly pointing to the GR. Before the analysis, the time-series data of each variable from each site were standardized using Z-scores to exclude spatial differences across vegetation types and arid areas. Chi-squared and Fisher’s C were used to test the possible paths of the SEMs. A nonsignificant Fisher’s C ($p > 0.05$) indicates that the model fits the data well. The direct and indirect effects were estimated by the *semEff* package of R (<https://murphymv.github.io/semEff/>, accessed on 1 March 2023). The standardized effect sizes and confidence intervals were calculated by bootstrapping with 10,000.

3. Results

3.1. Response of Vegetation Growth Rate to Changes in SOS and Climate Factors

The analysis of the 268 site-years data at the 33 sites showed that in more than 80% of the study sites there existed significant and positive correlations between the SOS and growth rate during the green-up period, with $r = 0.33$ (Figure 2A and Figure S2A). The correlations between the SOS and shortwave radiation and between the SOS and temperature were significantly negative and positive, respectively, with $r > 0.22$ (Figure 2B,C and Figure S2B,C). In contrast, the soil water content was not related to SOS (Figure 2D and Figure S2D). Similar results from both vegetation types (deciduous broadleaf and evergreen needleleaf forests) were obtained (Figure S3A–D, Figure S4A–D, Figure S5A–D, and Figure S6A–D).

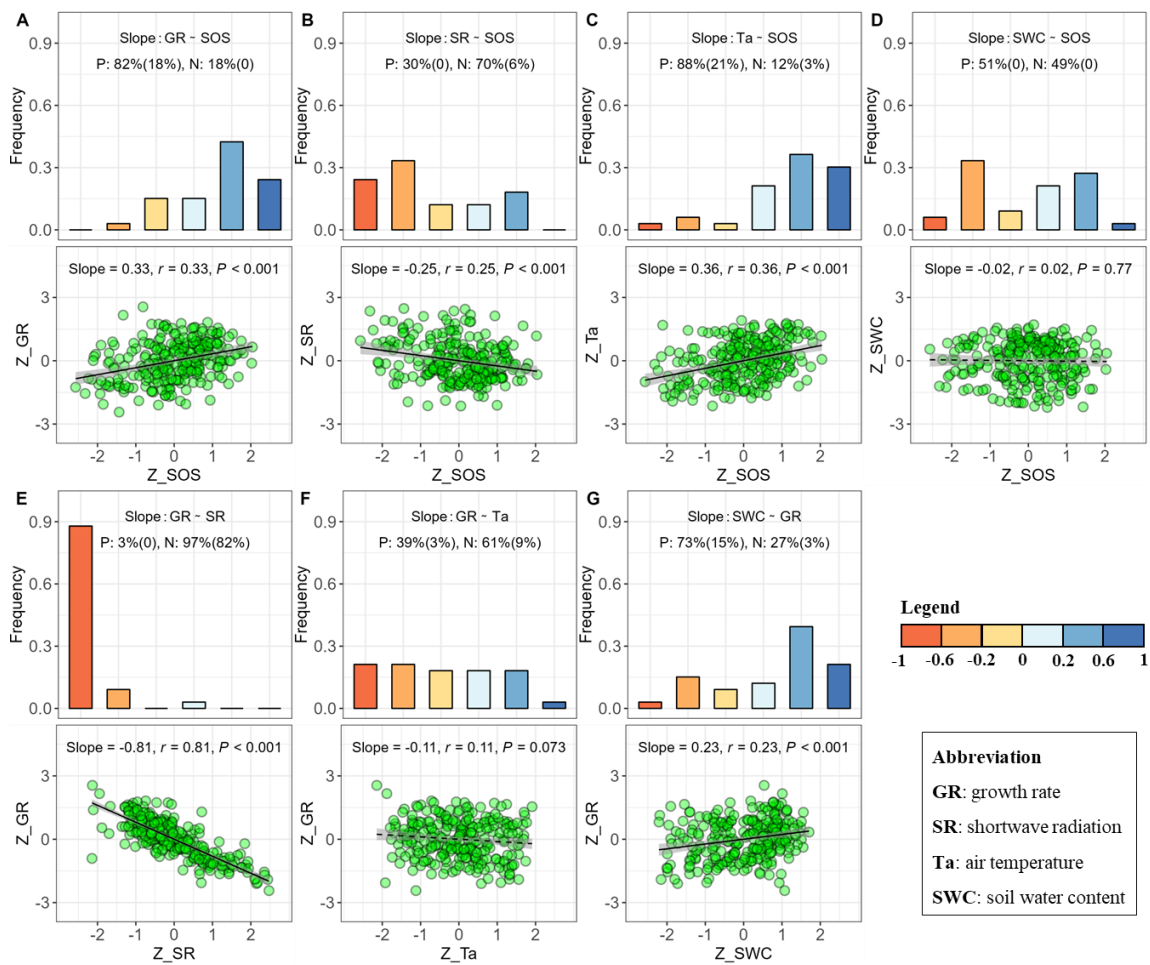


Figure 2. Frequency distributions and overall regression of site-level correlations of the start of the growing season (SOS) with the growth rate (GR, (A)), sum of shortwave radiation (SR, (B)), mean air temperature (Ta, (C)), and mean soil water content (SWC, (D)) during the green-up period, and the GR with SR (E), Ta (F) and SM (G). The percentages of areas of positive correlation (P) and negative correlation (N) are shown, and the significant percentages are displayed in parentheses. The results are derived from 268 year-site PhenoCam observations. The time-series data for each variable from each site were standardized using Z-scores. The extraction of SOS was based on the threshold method of 20%.

We also explored the changes in the vegetation growth rate with the climate factors and found that negative relationships between the growth rate and shortwave radiation accounted for more than 95% of the vegetated areas, with $r > 0.79$ (Figure 2E and Figure S2E). In contrast, the relationship between the growth rate and temperature was not significant,

and the correlation between the growth rate and soil water content was significantly positive, with $r > 0.21$ (Figure 2F,G and Figure S2F,G). We obtained similar results across the vegetation types (Figure S3E–G, Figure S4E–G, Figure S5E–G, and Figure S6E–G).

3.2. Effects of SOS on Growth Rate and Climate Factor Dependence on Aridity

The results of our study showed that an earlier-SOS-induced reduction in the growth rate was significantly weakened with an increasing aridity index, with slope < -0.48 and $r > 0.37$ (Figure 3A and Figure S7A). Similarly, an earlier-SOS-induced increase in shortwave radiation was significantly reduced with an increasing aridity index, with slope > 0.57 and $r > 0.37$ (Figure 3B and Figure S7B). The increase in the temperature with an earlier SOS slightly increased with an increasing aridity index, with slope > 0.20 and $r > 0.12$ (Figure 3C and Figure S7C), whereas the increase in the growth rate with temperature slightly decreased with an increasing aridity index, with slope > 0.27 and $r > 0.14$ (Figure 3F and Figure S7F). The effects of the SOS on soil water content, shortwave radiation on growth rate, and soil water content on growth rate had little changes with the aridity index (Figure 3D,E,G and Figure S7D,E,G).

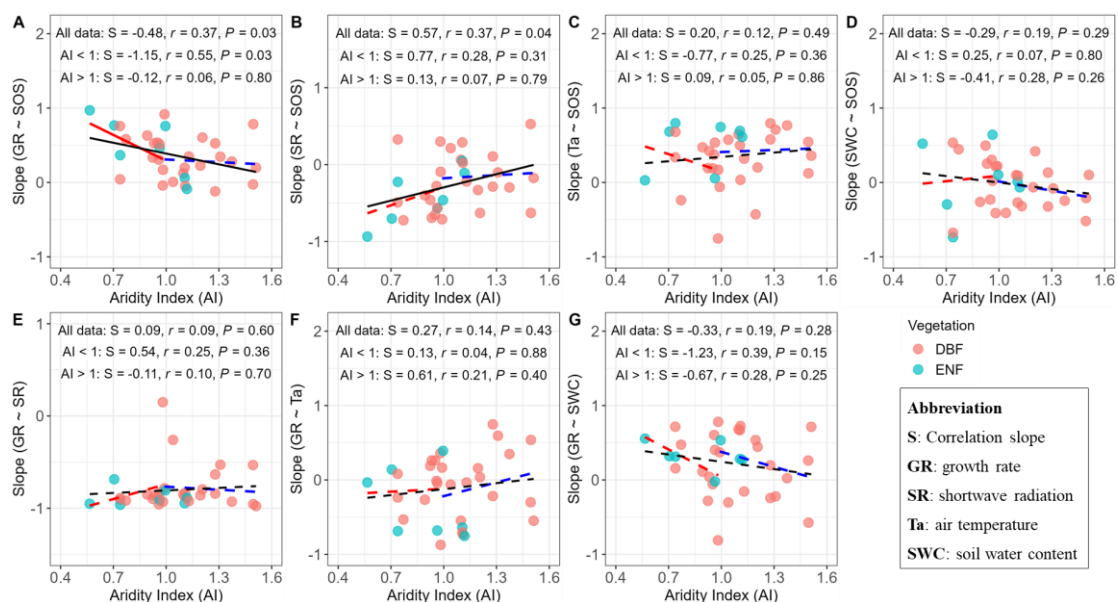


Figure 3. Changes in site-level slopes of the growth rate (GR, (A)), sum of shortwave radiation (SR, (B)), mean air temperature (Ta, (C)), mean soil water content (SWC, (D)) during the green-up period and the start of the growing season (SOS) with the aridity index, and site-level slopes of the SR (E), Ta (F), SM (G), and the GR with the aridity index. The solid line and dotted line indicate the significant and non-significant correlation between two variables, respectively. The red, blue, and black lines represent the results derived from $AI < 1$, $AI \geq 1$, and all data, respectively. The results are derived from 268 year-site PhenoCam observations. The time-series data for each variable from each site were standardized using Z-scores. Lower aridity index values correspond to drier climatic conditions. DBF, deciduous broadleaf forest; ENF, evergreen needleleaf forest. The extraction of SOS was based on the threshold method of 20%.

Interestingly, the effect of an earlier SOS on the growth rate was significantly reduced with an increasing aridity index in the humid areas (aridity index < 1), but it had little change in the highly humid areas (aridity index ≥ 1) (Figure 3A and Figure S7A). We also found that an earlier-SOS-induced increase in shortwave radiation had little change with an increasing aridity index in highly humid areas (aridity index ≥ 1) (Figure 3B and Figure S7B). Similarly, the differences in the effects of the SOS on the temperature and soil water content, and the effects of climate factors on the growth rate between the humid and highly humid areas were also detected (Figure 3C–G and Figure S7C–G).

3.3. Mechanisms of the Effects of SOS on Vegetation Growth Rate

The results of the structural equation models (SEMs) from all data revealed that an earlier SOS directly led to a low growth rate during the green-up period, and indirectly reduced the growth rate via an earlier-SOS-induced increase in the accumulative shortwave radiation and a decrease in the mean air temperature during the green-up period (Figure 4A, Figure S8A, and Figure S9). However, an earlier SOS had little influence on the mean soil water content during the green-up period (Figure S9), and we did not find an effect of the SOS on the vegetation growth rate via soil water content during the green-up period (Figure 4A and Figure S8A).

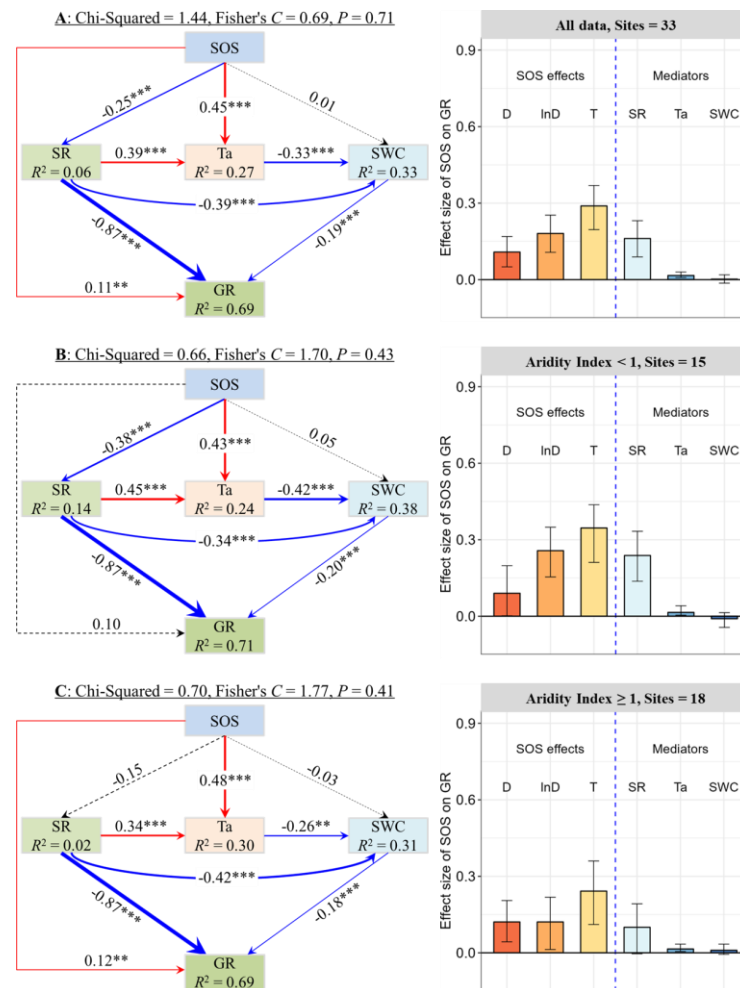


Figure 4. Structural equation models (SEMs) and the effect sizes of the start of the growing season (SOS) on vegetation growth rate (GR) through direct effects (SOS effects) and indirect effects via ‘mediator’ variables (mediators) for all data (A), the data with aridity index < 1 (B), and the data with aridity index ≥ 1 (C). D: direct effect; InD: indirect effect; T: total effect; SR: sum of shortwave radiation during the green-up period; Ta: mean air temperature during the green-up period; SWC: mean water content during the green-up period. The fitting parameters of SEMs are shown at the top of each SEM. The error bars in the histograms represent 95% confidence intervals. The solid line refers to a significant correlation between variables with $p < 0.01$ (**), and $p < 0.001$ (***). The red and blue lines indicate positive and negative relationships, respectively. The dotted or black line indicates a non-significant correlation between variables. The thickness of the lines indicates the strength of the correlation. The time-series data for each variable from each pixel of the SIF data were standardized using Z-scores. Lower aridity index values correspond to more arid climate conditions and vice versa. The extraction of SOS was based on the threshold method of 20%.

Importantly, the effects of an earlier SOS on the growth rate during the green-up period were different between the two arid areas (Figure 4B,C and Figure S8B,C). Specifically, an earlier SOS did not directly and significantly affect the growth rate, but it significantly reduced the growth rate via shortwave radiation and temperature in the humid areas with an aridity index < 1 (Figure 4B and Figure S8B). However, an earlier SOS not only directly and significantly reduced the growth rate, but it also significantly reduced the growth rate via temperature in the highly humid areas with an aridity index ≥ 1 (Figure 4C and Figure S8C).

4. Discussion

4.1. An Earlier SOS Induced Lower Vegetation Growth Rate

The vegetation growth rate plays a crucial role in regulating the ecosystem's productivity [8,9] and the economic value of ecosystems [34]. Previous research indicates that the vegetation growth rate showed a gradual increase at the decadal time scale [7,10,35]. In recent decades, most studies have proved that climatic warming has led to an advanced SOS in the time trends in temperate forests, although the temperature sensitivity of the SOS was reduced with ongoing warming [16]. These imply that an earlier SOS increases the vegetation growth rate over time [10]. However, one of the most striking results from our analyses was that an earlier SOS reduced the vegetation growth rate during the green-up period (Figure 2A and Figure S2A), which was different from the previous studies. This discrepancy may be because our study directly explored the effect of the SOS on the growth rate, and the interannual variation of the SOS is larger than that in the time trends over a period, as the other studies have focused on [12]. Thus, our results suggest that the ongoing advancement of the SOS reduces the vegetation growth rate during the green-up period, likely partly counteracting the vegetation productivity under future climate warming [2].

Four mechanisms may contribute to the reduction in the growth rate by an earlier SOS: (1) An earlier SOS prolongs the length of the green-up period, and increases the frost damage to leaves, resulting in slow plant growth and a low vegetation growth rate [22]; (2) an earlier SOS raises evapotranspiration and lowers the spring soil water, and low soil water availability limits plant growth and decreases the vegetation growth rate during the green-up period [14,18]; (3) an earlier SOS reduces the mean temperature during the green-up period because of large variations in the SOS at the interannual scale, thus lower temperature leads to a lower vegetation growth rate [36]; (4) an earlier SOS improves the accumulation of shortwave radiation as well as vegetation respiratory action, and it limits the vegetation growth [37]. However, the effects of the SOS on the vegetation growth rate may diversify between different arid areas, because of the various environmental contexts.

4.2. Effects of SOS on Vegetation Growth Rate Depended on Aridity Index

The temperature and soil water availability are important driving factors for vegetation growth [15]. The results of our study showed that an earlier-SOS-induced decrease in the growth rate significantly increased with increasing aridity (Figure 3A and Figure S7A). Furthermore, the effect of an earlier SOS on the growth rate was significantly different between the humid areas (aridity index < 1) and the highly humid areas (aridity index ≥ 1). The possible explanation may be that earlier-SOS-induced changes in climatic factors are different under different aridity levels, driving diverse responses of the growth rate to changes in the SOS [13,38]. For example, the increased soil-water stress due to an earlier SOS is the main factor limiting the vegetation growth rate in semi-humid or humid areas, whereas decreased heat due to an earlier SOS limits the vegetation growth rate in highly humid areas [17,18,20].

We further explored the effects of an earlier SOS on climate factors and its changes with an increasing aridity index. We found that an earlier-SOS-induced increase in shortwave radiation significantly increased with increasing aridity, and its increased magnitude was larger in the humid areas (aridity index < 1) than that in the highly humid areas (aridity index ≥ 1) (Figure 3B and Figure S7B). This is likely because there is a lower

temperature and/or more precipitation in highly humid areas than in humid areas [14,20]. Thus, an earlier SOS induced a lower mean temperature and more soil water content during the green-up period in the highly humid areas due to the high cloud cover and low evapotranspiration, and then drove the various changes in the vegetation growth rate (Figure 3 and Figure S7).

4.3. Shortwave Radiation and Temperature Regulated the Effect of SOS on Vegetation Growth Rate

Using structural equation models, we further tested the potential mechanisms for the effects of SOS on the vegetation growth rate and found that an earlier SOS not only directly reduced the growth rate but also indirectly reduced the growth rate via shortwave radiation and temperature (Figure 4A and Figure S8A). As for the direct effect of the SOS on growth rate, an earlier SOS can result in a longer green-up period and slight changes in the vegetation productivity [11,14], thus a lower growth rate was associated with an earlier SOS. As for the indirect effect of the SOS on the vegetation growth rate, an earlier SOS extended the length of the green-up period [14], and improved the accumulation of shortwave radiation during the green-up. Some researches indicate that shortwave radiation could boost the vegetation respiratory action, although it also increases the vegetation carbon uptake [37], ultimately resulting in a lower daily vegetation productivity (growth rate). Thus, it is not surprising why an earlier-SOS-induced increase in shortwave radiation reduced the vegetation growth rate during the green-up period. Interestingly, an earlier SOS significantly increased the accumulation of shortwave radiation in humid areas, but not in highly humid areas.

Similar to previous studies [36], we also found that an earlier SOS reduced the mean air temperature during the green-up period, especially in the highly humid areas (Figure S9). These results were not contradictory with that of the global ongoing rising temperature in recent years, because the variation in the SOS is large at the interannual scale (i.e., earlier SOS) [12]. As a primary limiting factor for plant growth, reduced temperature indirectly regulates the effect of the SOS on the vegetation growth rate [15]. In contrast, an earlier SOS did not affect the soil water content and then controlled the vegetation growth rate. This result is not consistent with our hypothesis due to almost all study sites being located in humid/high humid areas (Table S1), and the soil water availability is enough during the green-up period [17,18]. Overall, our findings emphasized that an earlier SOS reduced the growth rate during the green-up period, especially in the humid areas which are relatively arid compared to the high humid areas.

5. Conclusions

Using site-level observations from the PhenoCam dataset in temperate forests, we demonstrated that an earlier SOS reduced the vegetation growth rate during the green-up period. The increased accumulation of shortwave radiation and decreased mean air temperature caused by an earlier SOS indirectly regulated the effect of the SOS on the vegetation growth rate. Interestingly, the reduction in the growth rate was significantly larger in the humid areas than in the highly humid areas. These findings indicated that the reductions in the early-season growth rates due to an earlier SOS would intensify under ongoing global warming and increasing aridity in the future. Our study provides important insights into the mediating effects of the vegetation growth rate on the terrestrial carbon cycle during global climatic warming. Our findings emphasize the need to consider the negative effects of an earlier SOS on the vegetation growth rate which may partly offset the current increase in the productivity of temperate forests due to future warming and drought conditions.

Supplementary Materials: The following supporting information can be downloaded at: <https://www.mdpi.com/article/10.3390/f14101984/s1>, Figure S1: The initial structural equation model.; Figure S2: Frequency distributions and overall regression of site-level correlations of the start of the growing season (SOS) with the growth rate (GR, A), sum of shortwave radiation (SR, B), mean air temperature (Ta, C) and mean soil water content (SWC, D) during the green-up period, and the GR

with SR (E), Ta (F) and SM (G); Figure S3: Frequency distributions and overall regression of site-level correlations of the start of the growing season (SOS) with the growth rate (GR, A), sum of shortwave radiation (SR, B), mean air temperature (Ta, C) and mean soil water content (SWC, D) during the green-up period, and the GR with SR (E), Ta (F) and SM (G) for deciduous broadleaf forests (DBF); Figure S4: Frequency distributions and overall regression of site-level correlations of the start of the growing season (SOS) with the growth rate (GR, A), sum of shortwave radiation (SR, B), mean air temperature (Ta, C) and mean soil water content (SWC, D) during the green-up period, and the GR with SR (E), Ta (F) and SM (G) for evergreen needleleaf forests (ENF); Figure S5: Frequency distributions and overall regression of site-level correlations of the start of the growing season (SOS) with the growth rate (GR, A), sum of shortwave radiation (SR, B), mean air temperature (Ta, C) and mean soil water content (SWC, D) during the green-up period, and the GR with SR (E), Ta (F) and SM (G) for deciduous broadleaf forests (DBF); Figure S6: Frequency distributions and overall regression of site-level correlations of the start of the growing season (SOS) with the growth rate (GR, A), sum of shortwave radiation (SR, B), mean air temperature (Ta, C) and mean soil water content (SWC, D) during the green-up period, and the GR with SR (E), Ta (F) and SM (G) for evergreen needleleaf forests (ENF); Figure S7: Changes in site-level slopes of the growth rate (GR, A), sum of shortwave radiation (SR, B), mean air temperature (Ta, C), mean soil water content (SWC, D) during the green-up period, and the start of the growing season (SOS) with the aridity index, and site-level slopes of the SR (E), Ta (F), SM (G), and the GR with the aridity index; Figure S8: Structural equation models (SEMs) and the effect sizes; Figure S9: Total effect size of SOS on accumulative shortwave radiation (SR), mean air temperature (Ta), mean soil water content (SWC) during the green-up period for all data; Table S1: Aridity index for each site, and the regression slope of site-level correlations of the start of the growing season (SOS) with the growth rate (GR), sum of shortwave radiation (SR), mean air temperature (Ta) and mean soil water content (SWC) during the green-up period.

Author Contributions: Z.L. and J.L. designed the research. B.W. and Z.L. performed the analysis. B.W., Z.L. and J.L. drafted the paper. B.W., Z.L., J.L., M.C., C.Z., G.D., P.Y. and J.H. contributed to the interpretation of the results and to the text. All authors have read and agreed to the published version of the manuscript.

Funding: This research was funded by the National Natural Science Foundation of China (42301028), and the Postdoctoral Science Foundation of China (2023M730280).

Data Availability Statement: The canopy greenness data was downloaded from PhenoCam Dataset v2.0 (https://daac.ornl.gov/VEGETATION/guides/PhenoCam_V2.html). The climate data was obtained from ERA5-land hourly dataset (<https://cds.climate.copernicus.eu/cdsapp#!/dataset/reanalysis-era5-land?tab=overview>). The aridity index data was derived from Global-AI_PET_v3 dataset (https://figshare.com/articles/dataset/Global_Aridity_Index_and_Potential_Evapotranspiration_ET0_Climate_Database_v2/7504448/4).

Acknowledgments: The authors would like to thank the Council of China National Natural Science and China Post-doctoral Science Foundation for their support in the project.

Conflicts of Interest: The authors declare no conflict of interest.

References

1. Fu, Y.H.; Liu, Y.; De Boeck, H.J.; Menzel, A.; Nijs, I.; Peaucelle, M.; Penuelas, J.; Piao, S.; Janssens, I.A. Three times greater weight of daytime than of night-time temperature on leaf unfolding phenology in temperate trees. *New Phytol.* **2016**, *212*, 590–597. [[CrossRef](#)] [[PubMed](#)]
2. Hu, Z.; Wang, H.J.; Dai, J.H.; Ge, Q.S.; Lin, S.Z. Stronger spring phenological advance in future warming scenarios for temperate species with a lower chilling sensitivity. *Front. Plant Sci.* **2022**, *13*, 830573. [[CrossRef](#)]
3. Piao, S.L.; Liu, Q.; Chen, A.; Janssens, I.A.; Fu, Y.; Dai, J.; Liu, L.; Lian, X.; Shen, M.; Zhu, X. Plant phenology and global climate change: Current progresses and challenges. *Glob. Change Biol.* **2019**, *25*, 1922–1940. [[CrossRef](#)] [[PubMed](#)]
4. Keenan, T.F.; Gray, J.; Friedl, M.A.; Toomey, M.; Bohrer, G.; Hollinger, D.Y.; Munger, J.W.; O’Keefe, J.; Schmid, H.P.; Sue-Wing, I.; et al. Net carbon uptake has increased through warming-induced changes in temperate forest phenology. *Nat. Clim. Change* **2014**, *4*, 598–604. [[CrossRef](#)]
5. Piao, S.L.; Ciais, P.; Friedlingstein, P.; Peylin, P.; Reichstein, M.; Luysaert, S.; Margolis, H.; Fang, J.; Barr, A.; Chen, A.; et al. Net carbon dioxide losses of northern ecosystems in response to autumn warming. *Nature* **2008**, *451*, 49–52. [[CrossRef](#)]

6. Buermann, W.; Forkel, M.; O'Sullivan, M.; Sitch, S.; Friedlingstein, P.; Haverd, V.; Jain, A.K.; Kato, E.; Kautz, M.; Lienert, S.; et al. Widespread seasonal compensation effects of spring warming on northern plant productivity. *Nature* **2018**, *562*, 110–114. [[CrossRef](#)] [[PubMed](#)]
7. Wang, L.; Tian, F.; Wang, Y.; Wu, Z.; Schurgers, G.; Fensholt, R. Acceleration of global vegetation greenup from combined effects of climate change and human land management. *Glob. Change Biol.* **2018**, *24*, 5484–5499. [[CrossRef](#)]
8. Xia, J.Y.; Niu, S.L.; Ciais, P.; Janssens, I.A.; Chen, J.Q.; Ammann, C.; Arain, A.; Blanken, P.D.; Cescatti, A.; Bonal, D.; et al. Joint control of terrestrial gross primary productivity by plant phenology and physiology. *Proc. Natl. Acad. Sci. USA* **2015**, *112*, 2788–2793. [[CrossRef](#)]
9. Fu, Z.; Stoy, P.C.; Poulter, B.; Gerken, T.; Zhang, Z.; Waktulcho, G.; Niu, S.L. Maximum carbon uptake rate dominates the interannual variability of global net ecosystem exchange. *Glob. Change Biol.* **2019**, *25*, 3381–3394. [[CrossRef](#)]
10. Piao, S.L.; Wang, J.W.; Li, X.Y.; Xu, H.; Zhang, Y.C. Spatio-temporal changes in the speed of canopy development and senescence in temperate China. *Glob. Change Biol.* **2022**, *28*, 7366–7375. [[CrossRef](#)]
11. Wang, H.; Liu, H.Y.; Cao, G.M.; Ma, Z.Y.; Li, Y.K.; Zhang, F.W.; Zhao, X.; Zhao, X.Q.; Jiang, L.; Sanders, N.J.; et al. Alpine grassland plants grow earlier and faster but biomass remains unchanged over 35 years of climate change. *Ecol. Lett.* **2020**, *23*, 701–710. [[CrossRef](#)]
12. Marques, L.; Hufkens, K.; Bigler, C.; Crowther, T.W.; Zohner, C.M.; Stocker, B.D. Acclimation of phenology relieves leaf longevity constraints in deciduous forests. *Nat. Ecol. Evol.* **2023**, *7*, 198–204. [[CrossRef](#)]
13. Ren, P.; Ziaco, E.; Rossi, S.; Biondi, F.; Prislán, P.; Liang, E. Growth rate rather than growing season length determines wood biomass in dry environments. *Agr. Forest Meteorol.* **2019**, *271*, 46–53. [[CrossRef](#)]
14. Gao, S.; Liang, E.Y.; Liu, R.S.; Babst, F.; Camarero, J.J.; Fl, Y.H.; Piao, S.L.; Rossi, S.; Shen, M.G.; Wang, T.; et al. An earlier start of the thermal growing season enhances tree growth in cold humid areas but not in dry areas. *Nat. Ecol. Evol.* **2022**, *6*, 397–404. [[CrossRef](#)] [[PubMed](#)]
15. Liu, Z.C.; Zhang, S.M.; Lock, T.R.; Kallenbach, R.L.; Yuan, Z.Y. Aridity determines the effects of warming on community stability in Inner Mongolian grassland. *Agr. Forest Meteorol.* **2023**, *329*, 109274. [[CrossRef](#)]
16. Fu, Y.S.; Zhao, H.; Piao, S.; Peaucelle, M.; Peng, S.; Zhou, G.; Ciais, P.; Huang, M.; Menzel, A.; Uelas, J.P.; et al. Declining global warming effects on the phenology of spring leaf unfolding. *Nature* **2015**, *526*, 104–107. [[CrossRef](#)]
17. Liu, Z.C.; Fu, Y.H.; Shi, X.R.; Lock, T.R.; Kallenbach, R.L.; Yuan, Z.Y. Soil moisture determines the effects of climate warming on spring phenology in grasslands. *Agr. Forest Meteorol.* **2022**, *323*, 109039. [[CrossRef](#)]
18. Lian, X.; Piao, S.; Li, L.Z.X.; Li, Y.; Huntingford, C.; Ciais, P.; Cescatti, A.; Janssens, I.A.; Penuelas, J.; Buermann, W.; et al. Summer soil drying exacerbated by earlier spring greening of northern vegetation. *Sci. Adv.* **2020**, *6*, eaax0255. [[CrossRef](#)] [[PubMed](#)]
19. Wolf, S.; Keenan, T.F.; Fisher, J.B.; Baldocchi, D.D.; Desai, A.R.; Richardson, A.D.; Scott, R.L.; Law, B.E.; Litvak, M.E.; Brunsell, N.A.; et al. Warm spring reduced carbon cycle impact of the 2012 US summer drought. *Proc. Natl. Acad. Sci. USA* **2016**, *113*, 5880–5885. [[CrossRef](#)]
20. Zhang, Y.C.; Piao, S.L.; Sun, Y.; Rogers, B.M.; Li, X.Y.; Lian, X.; Liu, Z.H.; Chen, A.P.; Penuelas, J. Future reversal of warming-enhanced vegetation productivity in the Northern Hemisphere. *Nat. Clim. Change* **2022**, *12*, 581–586. [[CrossRef](#)]
21. Liu, Z.C.; Liu, K.; Shi, X.R.; Lock, T.R.; Kallenbach, R.L.; Yuan, Z.Y. Changes in grassland phenology and growth rate, rather than diversity, drive biomass production after fire. *Agr. Forest Meteorol.* **2022**, *322*, 109028. [[CrossRef](#)]
22. Liu, Q.; Piao, S.; Janssens, I.A.; Fu, Y.; Peng, S.; Lian, X.; Ciais, P.; Myneni, R.B.; Penuelas, J.; Wang, T. Extension of the growing season increases vegetation exposure to frost. *Nat. Commun.* **2018**, *9*, 426. [[CrossRef](#)]
23. Seyednasrollah, B.; Young, A.M.; Hufkens, K.; Milliman, T.; Friedl, M.A.; Frolking, S.; Richardson, A.D. Tracking vegetation phenology across diverse biomes using Version 2.0 of the PhenoCam Dataset. *Sci. Data* **2019**, *6*, 222. [[CrossRef](#)] [[PubMed](#)]
24. Richardson, A.D. Tracking seasonal rhythms of plants in diverse ecosystems with digital camera imagery. *New Phytol.* **2019**, *222*, 1742–1750. [[CrossRef](#)] [[PubMed](#)]
25. Keenan, T.F.; Darby, B.; Felts, E.; Sonnentag, O.; Friedl, M.A.; Hufkens, K.; O'Keefe, J.; Klosterman, S.; Munger, J.W.; Toomey, M.; et al. Tracking forest phenology and seasonal physiology using digital repeat photography: A critical assessment. *Ecol. Appl.* **2014**, *24*, 1478–1489. [[CrossRef](#)]
26. Sonnentag, O.; Hufkens, K.; Teshera-Sterne, C.; Young, A.M.; Friedl, M.; Braswell, B.H.; Milliman, T.; O'Keefe, J.; Richardson, A.D. Digital repeat photography for phenological research in forest ecosystems. *Agr. Forest Meteorol.* **2012**, *152*, 159–177. [[CrossRef](#)]
27. Filippa, G.; Cremonese, E.; Migliavacca, M.; Galvagno, M.; Forkel, M.; Wingate, L.; Tomelleri, E.; di Cella, U.M.; Richardson, A.D. Phenopix: A R package for image-based vegetation phenology. *Agr. Forest Meteorol.* **2016**, *220*, 141–150. [[CrossRef](#)]
28. Klosterman, S.T.; Hufkens, K.; Gray, J.M.; Melaas, E.; Sonnentag, O.; Lavine, I.; Mitchell, L.; Norman, R.; Friedl, M.A.; Richardson, A.D. Evaluating remote sensing of deciduous forest phenology at multiple spatial scales using PhenoCam imagery. *Biogeosciences* **2014**, *11*, 4305–4320. [[CrossRef](#)]
29. Zomer, R.J.; Xu, J.C.; Trabucco, A. Version 3 of the Global Aridity Index and Potential Evapotranspiration Database. *Sci. Data* **2022**, *9*, 409. [[CrossRef](#)]
30. Hong, S.B.; Ding, J.Z.; Kan, F.; Xu, H.; Chen, S.Y.; Yao, Y.T.; Piao, S.L. Asymmetry of carbon sequestrations by plant and soil after forestation regulated by soil nitrogen. *Nat. Commun.* **2023**, *14*, 3196. [[CrossRef](#)]
31. Uscanga, A.; Bartlein, P.J.; Silva, L.C.R. Local and regional effects of land-use intensity on aboveground biomass and tree diversity in tropical montane cloud forests. *Ecosystems* **2023**. [[CrossRef](#)]

32. Shipley, B. Confirmatory path analysis in a generalized multilevel context. *Ecology* **2009**, *90*, 363–368. [[CrossRef](#)] [[PubMed](#)]
33. Lefcheck, J.S. PIECEWISESEM: Piecewise structural equation modelling in R for ecology, evolution, and systematics. *Methods Ecol. Evol.* **2016**, *7*, 573–579. [[CrossRef](#)]
34. Pisani, D.; Paziienza, P.; Perrino, E.V.; Caporale, D.; De Lucia, C. The economic valuation of ecosystem services of biodiversity components in protected areas: A review for a framework of analysis for the Gargano national park. *Sustainability* **2021**, *13*, 53. [[CrossRef](#)]
35. Perrino, E.V.; Tomaselli, V.; Wagensommer, R.P.; Silletti, G.N.; Esposito, A.; Stinca, A. *Ophioglossum lusitanicum* L.: New Records of Plant Community and 92/43/EEC Habitat in Italy. *Agronomy* **2022**, *12*, 3188. [[CrossRef](#)]
36. Marchin, R.M.; McHugh, I.; Simpson, R.R.; Ingram, L.J.; Balas, D.S.; Evans, B.J.; Adams, M.A. Productivity of an Australian mountain grassland is limited by temperature and dryness despite long growing seasons. *Agr. Forest Meteorol.* **2018**, *256*, 116–124. [[CrossRef](#)]
37. Wu, Z.F.; Chen, S.Z.; De Boeck, H.J.; Stenseth, N.C.; Tang, J.; Vitasse, Y.; Wang, S.X.; Zohner, C.; Fu, Y.S.H. Atmospheric brightening counteracts warming-induced delays in autumn phenology of temperate trees in Europe. *Global Ecol. Biogeogr.* **2021**, *30*, 2477–2487. [[CrossRef](#)]
38. Montgomery, R.A.; Rice, K.E.; Stefanski, A.; Rich, R.L.; Reich, P.B. Phenological responses of temperate and boreal trees to warming depend on ambient spring temperatures, leaf habit, and geographic range. *Proc. Natl. Acad. Sci. USA* **2020**, *117*, 10397–10405. [[CrossRef](#)] [[PubMed](#)]

Disclaimer/Publisher’s Note: The statements, opinions and data contained in all publications are solely those of the individual author(s) and contributor(s) and not of MDPI and/or the editor(s). MDPI and/or the editor(s) disclaim responsibility for any injury to people or property resulting from any ideas, methods, instructions or products referred to in the content.